Ionization and Solubility of Chitosan Solutions Related to Thermosensitive Chitosan/Glycerol-Phosphate Systems

Dominic Filion,† Marc Lavertu,† and Michael D. Buschmann*

Institute of Biomedical Engineering, Department of Chemical Engineering, Ecole Polytechnique de Montreal, P.O. Box 6079, Station Centre-Ville, Montreal, Québec H3C 3A7, Canada

Received May 11, 2007; Revised Manuscript Received July 12, 2007

Chitosan is a linear cationic biopolymer composed of glucosamine and *N*-acetyl-glucosamine that is only soluble in acidic aqueous solutions and precipitates when neutralized. However, it was recently discovered that chitosan dissolved in solutions containing glycerol phosphate was soluble at near neutral pH and produced a sol−gel transition when heated. Understanding this unique thermogelling system requires improved characterization of the ionization and solubility behaviors of chitosan, in particular dependencies on temperature, salt, chitosan concentration, and f_D, where f_D is the fraction of glucosamine monomers (deacetylated monomers) in chitosan. In the current study we performed temperature-controlled titration and dilution experiments on chitosan solutions with f_D of 0.72, 0.85, and 0.98 at concentrations ranging from 1.875 to 30 mM of its glucosamine monomer and with 0 to 150 mM added salt. Light transmittance measurements were performed during titration to indicate precipitation. We found the apparent proton dissociation constant of chitosan, pK_{ap}, to (1) decrease strongly with increased temperature, (2) increase strongly with increased salt, (3) increase strongly with increased chitosan concentration in low-salt conditions, and (4) decrease weakly with increasing f_D. All of the above influences on chitosan pK_{ap} were accurately predicted using a mean-field Poisson−Boltzmann (PB) cylindrical cell model where the only adjustable parameter was the temperature-dependent chitosan intrinsic monomeric dissociation constant $pK_0(T)$. The resulting chitosan pK_0 values at 25 °C were in the range from 6.63 to 6.78 for all chitosans and salt contents tested. The temperature dependence of chitosan ionization was found to strongly reduce $pK_0(T)$ by 0.023 units per °C, for example, resulting in a reduction of chitosan $pK_0(T)$ from 7.1 at 5 °C to 6.35 at 37 °C for f_D of 0.72 in 150 mM salt. A similar temperature-dependent reduction of the pK_a of the glucosamine monomer was found (−0.027 units per °C) while the pK_a of glycerol phosphate did not change significantly with temperature. The latter result suggested that chitosan solutions heated in the presence of glycerol phosphate will become partly neutralized by transferring protons to glycerol phosphate and thereby allow attractive interchain forces to form a physically cross-linked gel under the appropriate conditions. Additionally, the degree of ionization of chitosan when it precipitates upon addition of a strong base was measured to be in the range from 0.25 to 0.55 and was found to (1) be insensitive to temperature, (2) increase strongly with increased salt, and (3) increase strongly with f_D. The salt effect was accounted for by the PB model, while the influence of f_D appeared to be due to acetyl groups impeding attractive chain-to-chain association to increase solubility and require reduced ionization levels to precipitate.

Introduction

Chitosan is a linear cationic polyelectrolyte derived by alkaline deacetylation of chitin in crustacean shells[1] and is composed of glucosamine and *N*-acetyl-glucosamine monomers linked by β-(1→4) glycosidic bonds. The fraction of monomers that are glucosamine is defined as f_D (fraction of deacetylated monomers). Chitosan possesses beneficial biological properties including biodegradability[2] and low toxicity[3,4] and can be used in drug delivery, gene delivery,[5−7] and wound healing.[8,9] Recently, a thermosensitive gelling system based on chitosan solutions buffered with glycerol phosphate (chitosan/GP)[10] was discovered and has been successfully applied to improve repair of lesions in articular cartilage.[11] Nonetheless, a satisfactory understanding of chitosan/GP solution properties, solubility, and thermosensitive characteristics is lacking. To fill this void, studies are required to examine chitosan ionization[12−20] and solubility behavior,[17,18,21] including dependencies on ionic strength, chitosan concentration and degree of deacetylation, and temperature.

Potentiometric titration is widely used to investigate polyelectrolyte behavior in solution. Previous studies have reported titration[12−19] and precipitation[20,21] behavior of chitosan during neutralization. However, no molecular scale theoretical model was proposed or tested to predict chitosan titration nor has work to date investigated the particular influence of temperature on chitosan ionization. The objective of the current study was therefore to examine chitosan ionization and solubility behavior as a function of ionic strength, f_D, chitosan concentration, and temperature. A second objective was to assess the ability of the nonlinear Poisson−Boltzmann cylindrical cell model to predict the apparent dissociation constant of chitosan at finite concentration, its pK_{ap}, and the pK_{ap} dependence on chitosan ionization, level of deacetylation, concentration of chitosan, medium ionic strength, and temperature. Use of this model to predict the polyelectrolyte titration behavior was pioneered by Kotin and Nagasawa.[22] We performed titration and dilution experiments simultaneously measuring laser light transmittance

* Author to whom correspondence should be addressed. Phone: (514) 340-4711 ext 4931. Fax: (514) 340-2980. E-mail: michael.buschmann@polymtl.ca.

† These authors contributed equally to this work.

10.1021/bm700520m CCC: $37.00
Published on Web 09/13/2007

(L_T) to detect precipitation of chitosan solutions at different but constant temperatures ranging from 5 to 37 °C. Solutions of chitosan with f_D ranging from 0.72 to 0.98 and with the mono-monovalent salt concentration ranging from 0 to 150 mM were titrated, and the resulting data were analyzed using a nonlinear Poisson−Boltzmann cylindrical cell model. We hypothesized that (i) increased ionic strength would dampen ionization-dependent behavior via electrostatic screening and decrease chitosan solubility, (ii) that increased f_D would increase solubility and reduce apparent pK_a via increased electrostatic repulsion, (iii) that increasing the concentration of chitosan in solution would increase apparent pK_a by flattening intermolecular electrostatic potential profiles, and (iv) that increasing temperature would expel protons from chitosan and thereby reduce chitosan pK_{ap}.

We also performed temperature ramp experiments with simultaneous pH measurement on solutions of simple electrolytes including glucosamine (the ionizable subunit of chitosan) and GP, the anionic buffer present in chitosan/GP solutions. The goal here was to evaluate the contribution of the temperature-dependent ionization behavior of the monomer (glucosamine) toward behavior of the polymeric form (chitosan) and to examine the influence of temperature on GP ionization. We hypothesized that GP ionization may be relatively insensitive to temperature such that GP may act as an efficient acceptor of protons released from chitosan when chitosan/GP solutions are heated. Such a heat-induced transfer of protons from chitosan to GP would reduce the degree of ionization of chitosan and, therefore, chitosan intermolecular electrostatic repulsion, allowing attractive hydrophobic and hydrogen bonding interchain forces to initiate physical cross-linking, resulting in the formation of a gel in sufficiently concentrated solutions.

Theory

A cylindrical cell model representation of chitosan in solution was used to obtain a molecular electrostatic potential by solving the nonlinear Poisson−Boltzmann (PB) equation within the cylindrical cell.[23] The model was developed for solutions that contain the cationic polyelectrolyte, its anionic counterion (Cl^-), a strong base titrant (NaOH), and a monovalent salt (NaCl). The molecular electrostatic potential profile from a numerical solution was then used to predict titration pH curves as described below.

Structural Parameters of the Cylindrical Cell Model. Chitosan is composed of two distinct monomers: a fraction f_D of ionizable glucosamine and a fraction $1 - f_D$ of non-ionizable *N*-acetyl-glucosamine (Figure 1A). Chitosan is represented as an infinitely long impermeable cylinder of radius a (Figure 1B) where discrete charge sites are smeared out to form a uniform surface charge density σ

$$\sigma = \frac{e\alpha f_D}{2\pi a l} \tag{1}$$

where e is the elementary charge, α is the degree of ionization of the polycation ($\alpha = 0$ is neutral and $\alpha = 1$ is fully ionized), and l is the length of the monomer that is set to $l = 0.52$ nm following structural data.[24,25] The radius of the inner cylinder representing chitosan is taken as $a = 1.3$ nm, even though this value is greater than what structural data suggest (0.42 nm),[24] an assumption that is elaborated upon below in the Discussion. Each polymer chain is located at the center of a cylindrical cell whose radius b (Figure 1B) is determined from the monomer concentration c_p (including both glucosamine and *N*-acetyl-glucosamine) and monomer length l, according to

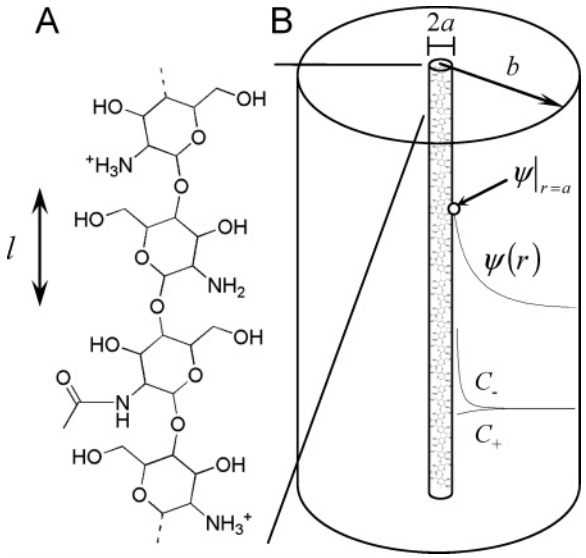

Figure 1. (A) A four monomer segment of chitosan represented with two protonated monomers, a neutral monomer, and a non-ionizable *N*-acetyl-glucosamine monomer. Each monomer has length l. (B) Cylindrical cell model showing the inner cylinder with radius a, representing a chitosan molecule that is contained in its electrolyte envelope extending to radius b, which is determined by chitosan concentration (eq 2). Representative profiles of electrostatic potential $\psi(r)$, counterion concentration, c_-, and co-ion concentration, c_+ are shown for the case of $c_{NaCl} = 15$ mM at $\alpha = 0.75$ and $f_D = 1.00$. The circle indicates the electrostatic potential at the surface of the polyelectrolyte, $\psi_{r=a}$.

$$b = \left(\frac{1}{\pi l c_p N_A}\right)^{1/2} \tag{2}$$

where N_A is Avogadro's number.

Counterion and Co-ion Molecular Scale Concentration Profiles, Average Macroscopic Values, and Activities. The polycation is surrounded by mobile ions in the region $a < r < b$. Using the mean-field approximation,[23] these ions are assumed to follow a Boltzmann distribution at equilibrium, resulting in a concentration profile $c_i(r)$ for mobile ion i about the polyion that is a function of radial position r and electrostatic potential $\psi(r)$

$$c_i(r) = c_i^0 \, e^{-z_i e\psi(r)/kT} \tag{3}$$

where z_i is the valence of the mobile ion i, T is the temperature, and k is Boltzmann's constant. The value of c_i^0 is related to the mean concentration of positive and negative electrolyte ions, $\bar{c}_\pm$, in the volume of the cylindrical cell according to

$$\bar{c}_\pm = c_\pm^0 \frac{\int_a^b 2r \, e^{\mp e\psi(r)/kT} \, dr}{b^2} = \frac{c_\pm^0}{\gamma_\pm} \tag{4}$$

where a mono-monovalent electrolyte, $z_i = +1$ or -1, is considered. $\gamma_\pm = b^2/\int_a^b 2r \, e^{\mp e\psi(r)/kT} \, dr$ are the mobile ion activity coefficients in the cylindrical cell and $\gamma_\pm \bar{c}_\pm = c_\pm^0$ are ion activities ($a_\pm = \gamma_\pm \bar{c}_\pm = c_\pm^0$) as derived previously[23] for this particular mean-field theory.

Poisson−Boltzmann Equation. The electrostatic potential, ψ ($a < r < b$), can be found from the solution to the Poisson−Boltzmann equation[26−28] in cylindrical coordinates

$$\frac{d^2\psi(r)}{dr^2} + \frac{1}{r}\frac{d\psi(r)}{dr} = -\frac{\rho(r)}{\epsilon} = -\frac{\sum_i z_i e c_i^0 \, e^{-z_i e\psi(r)/kT}}{\epsilon} \quad (5)$$

subject to boundary conditions from Gauss' law

$$\left.\frac{d\psi(r)}{dr}\right|_{r=a} = -\frac{\sigma}{\epsilon} = -\frac{e\alpha f_D}{2\pi a l \epsilon} \quad \text{and} \quad \left.\frac{d\psi(r)}{dr}\right|_{r=b} = 0 \quad (6)$$

where ϵ is the permittivity of water and $\rho(r)$ is the spatially varying charge density. The solution to eq 5 must also satisfy eq 4 since the polyelectrolyte solution is contained in a closed volume with known total mobile ion concentrations rather than in contact with an infinite bath.

We now demonstrate that the choice of reference electric potential is arbitrary. If we add a constant C to a solution, $\psi_{sol}(r)$, of eqs 4−6, then this new function, $\psi_{sol}(r) + C$, clearly satisfies the boundary conditions of eq 6 since only derivatives of the potential appear in eq 6. However, to satisfy eq 4, the mobile ion activities, i.e., c_-^0 and c_+^0, must change to $c_-^0 \, e^{-eC/kT}$ and $c_+^0 \, e^{+eC/kT}$, respectively. Finally, inserting $\psi_{sol}(r) + C$ into eq 5 written for a mono-monovalent electrolyte and using $c_-^0 \, e^{-eC/kT}$ and $c_+^0 \, e^{+eC/kT}$ for c_-^0 and c_+^0 we find

$$\frac{d^2(\psi_{sol}(r)+C)}{dr^2} + \frac{1}{r}\frac{d(\psi_{sol}(r)+C)}{dr} =$$
$$\frac{d^2\psi_{sol}(r)}{dr^2} + \frac{1}{r}\frac{d\psi_{sol}(r)}{dr} = \frac{e}{\epsilon}(c_-^0 \, e^{-eC/kT} \, e^{+e(\psi_{sol}(r)+C)/kT} -$$
$$c_+^0 \, e^{+eC/kT} \, e^{-e(\psi_{sol}(r)+C)/kT}) =$$
$$\frac{e}{\epsilon}(c_-^0 \, e^{+e\psi_{sol}(r)/kT} - c_+^0 \, e^{-e\psi_{sol}(r)/kT}) \quad (7)$$

showing that $\psi_{sol}(r) + C$ satisfies the PB equation and boundary conditions as well as the known content of mobile ions in the closed solution, as long as c_-^0 and c_+^0 become $c_-^0 \, e^{-eC/kT}$ and $c_+^0 \, e^{+eC/kT}$, respectively. This result also reveals the interesting conclusion that there always exists a reference potential (value of C) for which mobile ion activities are equal, $c_-^0 = c_+^0$.

In the context of this study, we consider three types of mobile ions, namely, the counterion Cl^- (from the solvent HCl and NaCl salt added), the co-ion Na^+ (from the dissociation of NaOH and NaCl), and protons (H^+). Hydroxyl ions (OH^-) are neglected since only acidic solutions are considered. To facilitate numerical solution of eq 5, we choose to equate total counterion and co-ion activities

$$c_{Cl}^0 = c_{Na}^0 + c_H^0 = c^0 \quad (8)$$

which simply implies a particular value of reference potential, or C, as described above. Note that Na^+ and H^+ can be grouped together as they are both monovalent cations following the same Boltzmann distribution. Equation 5 can then be rewritten in terms of c^0 alone, using eq 8, to obtain

$$\frac{d^2\psi(r)}{dr^2} + \frac{1}{r}\frac{d\psi(r)}{dr} = \frac{2ec^0}{\epsilon}\sinh\left(\frac{e\psi(r)}{kT}\right) \quad (9)$$

For a given α that defines the polyelectrolyte surface charge σ according to eq 1, and a given polyelectrolyte monomer concentration c_p, which defines the outer cell radius b according to eq 2, we numerically solved eq 9 such that the boundary conditions of eq 6 are satisfied. An initial guess for c^0 was taken, and the solution was then iterated with different values of c^0 until the right-hand side of eq 4 converged to the experimentally known average ion concentrations, $\bar{c}_\pm$. In this way the Poisson−Boltzmann equation was solved for a closed volume of polyelectrolyte solution at finite concentration that is not in equilibrium with an external bath. The numerically obtained solution for $\psi(r)$ was then finally adjusted by subtracting from it the value found for $\psi(b)$ to redefine the reference potential as $\psi(b) = 0$, which has no physical consequence, but conforms to the reference potential used to derive eq 11 below in Appendix 1 of the Supporting Information. This reference potential also conveniently redefines $c_\pm^0$ as the ion concentrations at $r = b$, in addition to the ion activity $a_\pm$ in the polyelectrolyte fluid phase.

Theoretical Dependence of pH on pK_0, α, and $\psi|_{r=a}$. The pH is related to proton activity, a_H, in the fluid phase via

$$pH = -\log_{10} a_H = -\log_{10} \gamma_+ \bar{c}_H = -\log_{10} c_H{}^0 \quad (10)$$

where the right most term contains the proton concentration, c_H^0, at the cylindrical cell boundary, $r = b$, where $\psi(r = b) = 0$ and $d\psi(r = b)/dr = 0$, allowing these protons to behave ideally. By equating the chemical potential of protons in the fluid phase to that of the polyelectrolyte chain, a theoretical relationship for pH as a function of pK_0, α, and $\psi_{r=a}$, the electrostatic potential at the surface of the polyelectrolyte in the Poisson−Boltzmann cylindrical cell model was derived (eq 35 in Appendix 1 of the Supporting Information; see also Marcus[23] for a similar derivation) as

$$pH = pK_0(T) + \log_{10}\frac{1-\alpha}{\alpha} - \frac{e\psi|_{r=a}}{kT\ln 10} \quad (11)$$

where p$K_0(T)$ is the intrinsic dissociation constant of the glucosamine monomer of chitosan. A useful expression to compare with experiments is the apparent pK_a, or pK_{ap}

$$pK_{ap}(T) = pH(T) - \log_{10}\frac{1-\alpha}{\alpha} = pK_0(T) - \frac{e\psi|_{r=a}}{kT\ln 10} \quad (12)$$

that includes two contributions, the first representing the intrinsic monomeric dissociation constant p$K_0(T)$ and the second containing the polyelectrolyte surface potential $\psi|_{r=a}$, which can be found by solving the Poisson−Boltzmann equation. Note that for simple acid−base- electrolytes $\psi|_{r=a} = 0$ in the current model so that the apparent pK_a (pK_{ap}) and pK_a become identical $pK_{ap}(T) = pK_0(T) = pK_a(T)$.

Electroneutrality and the Poisson−Boltzmann Equation Determine α and $\psi|_{r=a}$. The degree of ionization, α, is required to calculate pH from eq 11 and to initiate solution of the eq 9 to find $\psi|_{r=a}$, which is also required in eq 11. To determine α, we used the condition of macroscopic electroneutrality, again neglecting hydroxyl ions

$$\bar{c}_{Cl} - \bar{c}_{Na} - \bar{c}_H - c_g^+ = 0 \quad (13)$$

where c_g^+ is the concentration of ionized glucosamine monomers

$$c_g^+ = \alpha f_D c_p \quad (14)$$

Substituting eqs 10 and 14 into eq 13 we find

$$\alpha = \frac{\bar{c}_{Cl} - \bar{c}_{Na} - \frac{10^{-pH}}{\gamma_+}}{f_D c_p} \quad (15)$$

α and the corresponding $\psi|_{r=a}$ were determined for each particular experimental pH in titration and dilution experiments. In most cases, the proton concentration, $10^{-pH}/\gamma_+$, is negligible, and α is simply determined from the known ion and monomer concentrations (taking into account any dilution from the cumulative titrant addition). For cases where proton concentration must be considered, $10^{-pH}/\gamma_+$ can be estimated by using the experimental pH and assuming ideality for the protons $\gamma_+ = 1$, thus avoiding the need to simultaneously solve the Poisson Boltzmann equation to find α.

Determination of p$K_0(T)$ and of the Temperature Dependence of pK_{ap}. Once the values of $\psi|_{r=a}$ and α for each pH in a given titration curve are found as described above (for pH values in the soluble range of titration experiments), we subsequently insert these $\psi|_{r=a}$ and α values into eq 11 and fit eq 11 to pH data by adjusting p$K_0(T)$ to find the best fit value of p$K_0(T)$ for each temperature. Temperature-induced changes in pK_{ap} were directly derived from temperature-induced pH changes using the following relationship derived in Appendix 2 of the Supporting Information

$$dpK_{ap} = dpH + \frac{1}{\alpha(1-\alpha)}\left(\left(\frac{c_{H^+}}{c_g^t} + \frac{c_{OH^-}}{c_g^t}\right)dpH - \frac{c_{OH^-}}{c_g^t}\, dpK_{water}\right) \quad (16)$$

where c_{H^+} and c_{OH^-} are proton and hydroxyl ion concentrations, $c_g^t = f_D c_p$ is the total glucosamine monomer concentration and d pK_{water} is the dissociation constant of water. Equation 16 can be simplified to

$$dpK_{ap} \approx dpH \quad (17)$$

if

$$\frac{c_{H^+}}{c_g^t} \ll 1 \quad \text{and} \quad \frac{c_{OH^-}}{c_g^t} \ll 1 \quad (18)$$

and α is not too close to 0 or 1. These conditions were valid in our experiments where $c_g^t > 3$ mM and pH > 5 (corresponding to $\alpha < 0.75$) or pH > 5.3 (corresponding to $\alpha < 0.90$) for cases with 0 or 150 mM added salt, respectively. Under these conditions, the temperature-induced change in pK_{ap}, $\Delta pK_{ap}(T) = pK_{ap}(T) - pK_{ap}(T_{ref})$, with respect to that of an arbitrary reference temperature T_{ref}, can be determined from the corresponding pH difference via

$$\Delta pK_{ap}(T) = pK_{ap}(T) - pK_{ap}(T_{ref}) = pH(T) - pH(T_{ref}) \quad (19)$$

Experimental Methods

Reagents and Solutions. Ultrapure chitosans with f_D ranging from 0.72 to 0.98 were provided by BioSyntech (Table 1). These polymers have a number average molecular weight (M_n) ranging from 100 to 550 kDa and a polydispersity index (PDI = M_w/M_n) of 1.6−2.3. NaOH 1 N (Aldrich, catalogue no. 31951-1) and HCl 1 N (Aldrich, catalogue no. 31894-9) were used to prepare the titrant solution and to dissolve chitosan, respectively. Chitosan solutions with precise concentrations were prepared from powders dried at 60 °C for 2 days using a heated centrifugal vacuum concentrator (Savant Speedvac, model SS110) and kept in a desiccator until use.

Table 1. Characteristics of Chitosans

f_D	M_n [a] (kDa)	PDI [b]
0.72	553	2.3
0.85	226	1.7
0.98	103	1.6

[a] Number average molecular weight (M_n) by triple detector gel permeation chromatography.[29] [b] Polydispersity index (PDI = M_w/M_n) using weight average molecular weight (M_w) obtained by gel permeation chromatography, both provided by the manufacturer.

For titration experiments, chitosan was dissolved to obtain a 3 mM concentration of its glucosamine monomer in a 500 mL volumetric flask, and HCl was added to a molar ratio of HCl/glucosamine of 1:1 resulting in $\alpha \cong 0.97$ according to electroneutrality (eq 13) and using the resulting pH of the solution of about 4. To make these solutions, dried chitosan was added to deionized water, stirred to disperse the powder prior to adding HCl, and then stirred overnight to ensure complete dissolution. The NaCl concentration was adjusted by adding appropriate amounts of 5 M NaCl (Fisher Scientific, catalogue no. S271-1) resulting in a maximum dilution of glucosamine monomer and HCl to 2.91 mM at the highest level of added salt used of $c_{NaCl} = 150$ mM.

In experiments where chitosan was diluted rather than titrated to obtain concentration-dependent behavior, chitosan solutions corresponding to 30 mM glucosamine monomer were prepared in a manner similar to that described above but to obtain molar ratio of HCl/glucosamine of 0.75:1. The NaCl concentration was subsequently adjusted by adding appropriate amounts of 5 M NaCl. Chitosan solutions were then diluted while monitoring pH as described below from the initial 30 mM glucosamine monomer up to a dilution corresponding to 1.875 mM glucosamine monomer. Dilution was performed using each of the following conditions: (1) Chitosan without added salt was diluted with deionized water, (2) chitosan with excess salt of $c_{NaCl} = 300$ mM was diluted with deionized water, and (3) chitosan with $c_{NaCl} = 300$ mM was diluted with 300 mM NaCl. The variation of pK_{ap} during these dilution experiments corresponds to the recorded pH variation similar to eq 19, but with temperature replaced by concentration, since $\alpha = 0.75$ is constant throughout these experiments and proton concentrations are negligible.

Monomeric glucosamine (non-polyelectrolyte) solutions were also prepared by adding 12.9 mg D-(+)-glucosamine hydrochloride (Sigma, catalogue no. G1514) to 20 mL of distilled and deionized water to obtain 3.00 mM D-(+)-glucosamine with 3.00 mM Cl^- counterion. Further addition of 0.3 mL of 0.01 N NaOH solution produced a solution with $\alpha \cong 0.95$ that was used for temperature ramp tests described below. (Equation 17 is satisfied since pH > 5.8, and d pK_a/dpH = 1.00 ± 0.01.) Glycerol phosphate solutions at a concentration of 50 mM with $\alpha = 0.5$ were prepared by adding 297 mg of GP (Sigma, catalogue no. G9891) to 20 mL of distilled and deionized water followed by addition of 0.5 mL of 1 N HCl. (Equation 17 is satisfied since pH = 6.2 and d pK_a/dpH = 1.00 ± 0.01.)

Experimental Apparatus. A custom apparatus (Figure 2) allowed simultaneous measurement of pH and laser light relative transmittance (L_T), the latter used to detect precipitation of chitosan solutions. We used this apparatus for titration and dilution experiments of chitosan and to measure pH and pK_a of D-(+)-glucosamine, chitosan, and GP solutions during temperature ramp tests. Solutions were continuously stirred inside a 50 mL reaction jacketed beaker (Kontes, catalogue no. 317000-0050) with the jacket coupled to a heating circulating bath (Neslab, model RT-111) to control temperature via an automatic temperature compensation (ATC) probe (Accumet, Fisher Scientific catalogue no. 13-620-16) immersed in the tested solution. The pH electrode (Orion, model no. 8115 connected to the Accumet, model 20 pH meter) was calibrated with National Institute of Standards and Technology standards at room temperature, and the automatic ATC probe was corrected for the temperature dependence of the pH electrode. Addition of titrant was performed using an automatic burette (Schott,

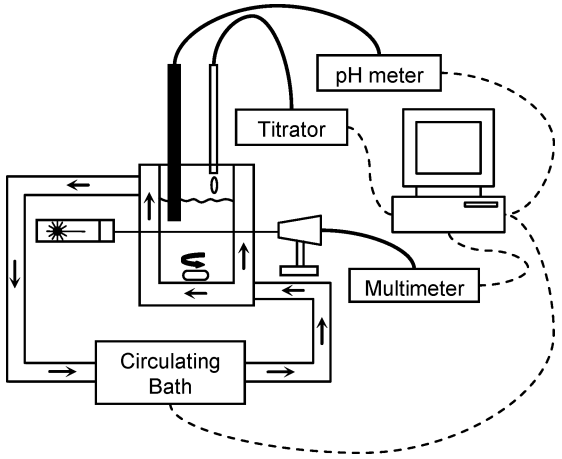

Figure 2. Custom experimental apparatus for temperature-controlled titration with simultaneous recording of temperature, pH, and relative light transmittance (L_T) of chitosan solutions. Solution temperature was controlled via the circulating bath, and a burette added 0.01 N NaOH for titration or deionized water or 300 mM NaCl for dilution experiments. A photodetector assesses laser light transmittance through the beaker and solution to detect chitosan precipitation.

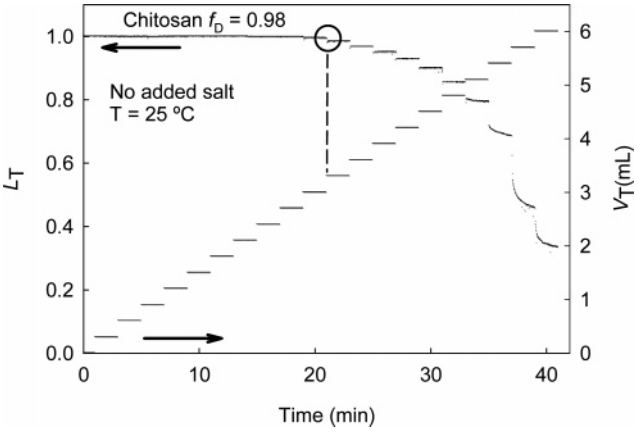

Figure 3. Relative light transmittance, L_T, and cumulative volume of added titrant, V_T, versus time illustrating the first step decrease in L_T (circle) due to chitosan precipitation occurring after 3.3 mL of 0.01 N NaOH has been added in this case. The α_p value was then calculated from eq 14, using the known Na^+, Cl^-, and c_p concentrations at the corresponding injection volume, neglecting the proton concentration.

Titronic Universal 20 mL), which added 0.3 mL increments of 0.01 N NaOH every 2 min for titration experiments; for dilution experiments either deionized water or 300 mM NaCl were added as described above. To detect chitosan precipitation, laser light relative transmittance, L_T, was measured throughout titration by passing a 635 nm diode laser beam (Coherent, 5 mW, 31-0128) through the solution and walls of the beaker with detection by a photo detector (Coherent, Laser-Q VIS, 33-0241 connected to a multimeter Fluke, model 45 dual display). The point of precipitation was characterized by a sharp decrease of L_T following injection of the titrant (as in Figure 3). The value of α at which these L_T values decreased to indicate precipitation was termed α_p. The computer controlled the titration burette and bath temperature in addition to acquiring pH, temperature, and L_T data.

Statistical Analysis. In this study, when presenting experimental data with error bars, the mean value with a confidence interval of one standard deviation (SD) and the number of independent measurements (n) are reported. For example, mean ± SD, $n = 3$, indicates that the mean of three measurements with a confidence interval of one standard deviation is reported. In the case where fit parameters are reported, the above also applies except that the SD now corresponds to the standard deviation of each fit parameter obtained with n independent fits, one for each measurement.

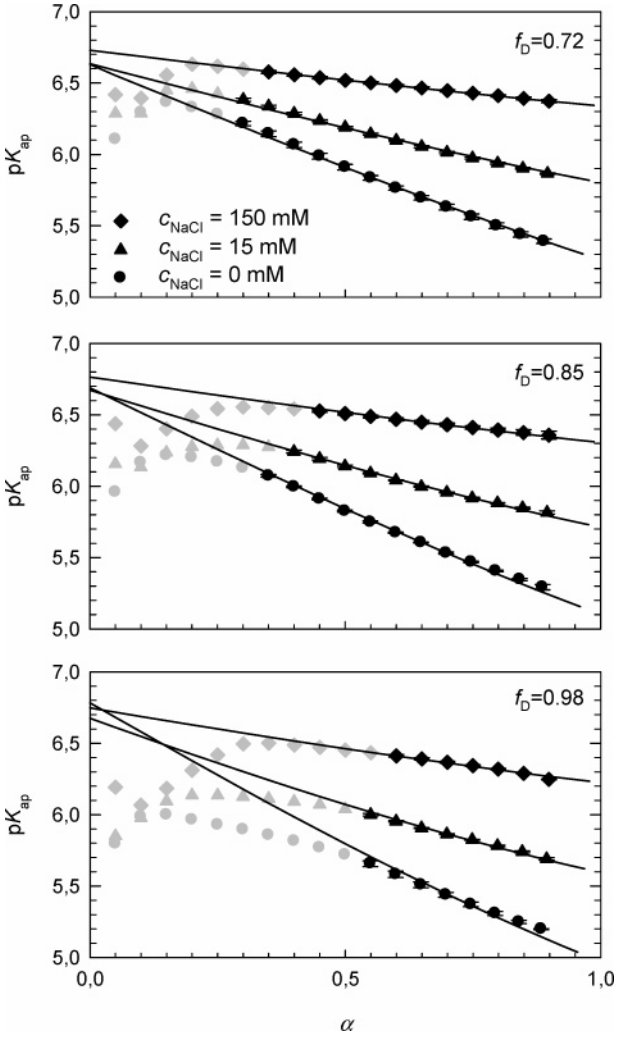

Figure 4. Dependence of chitosan pK_{ap} at 25 °C (mean ± SD, n = 3) on degree of ionization (α) for nine combinations of f_D and c_{NaCl} compared to best fits of the PB model (continuous lines). Gray symbols indicate data after chitosan precipitation. These PB model fits were obtained using a = 1.3 nm (polyelectrolyte radius) and l = 0.52 nm (charged sites spacing on the chain) and then adjusting pK_0-(T) for the best fit taking into account dilution from added titrant.

Results

Influence of Ionic Strength and Fraction of Deacetylation (f_D) on Titration (pK_{ap} and pK_0) and Precipitation (α_p) Behavior of Chitosan. In regions where the chitosan ionization state is relatively high ($\alpha > 0.5$), increasing ionic strength significantly increased chitosan pK_{ap} almost by a full unit upon addition of 150 mM salt (Figure 4). On the contrary, similar measurements of monomeric glucosamine displayed only a minimal increase in pK_a, indicating that the salt dependence of pK_{ap} of chitosan is due to modulation of the surface potential in the polyelectrolyte term, $-e\psi|_{r=a}/(kT \ln 10)$ of eq 12. This conclusion was also supported by the PB model predicting a strong decrease of the chitosan surface potential $\psi|_{r=a}$ as ionic strength increased (Figure 5A) and by the ability of this model to capture titration behavior (Figure 4). The degree of ionization of chitosan at the point of precipitation, α_p, increased with increasing ionic strength (Table 2), presumably due to increased electrostatic screening (Figure 5A) allowing for readier inter-chain association.

Increasing f_D produced only a slight reduction in pK_{ap} (Figure 6) that was also consistent with the PB model showing a slight

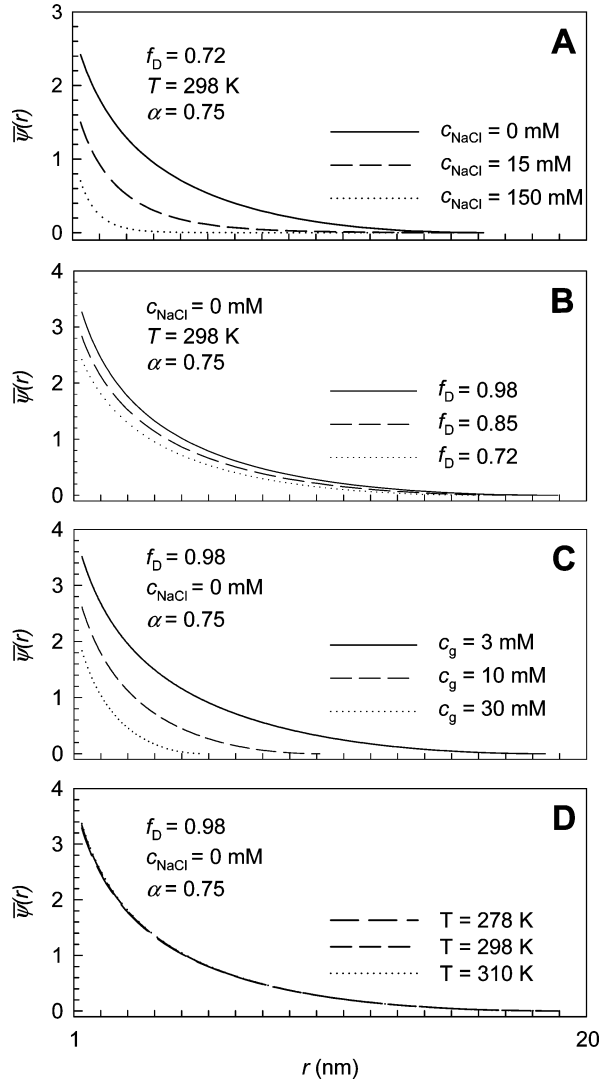

Figure 5. Normalized electrostatic potential profile $\bar{\psi}(r) = e\psi(r)/kT$ calculated from the Poisson−Boltzmann cylindrical cell model from the surface of chitosan ($r = a = 1.3$ nm for our calculations) out to the midpoint between two adjacent chitosan molecules at $r = b$. The outer radius b varies with concentration in part C, according to eq 2, and with α due to titrant dilution. Note however that b also varies with f_D in part B since total glucosamine monomer initial concentration was kept constant at 3.0 mM rather than keeping c_p constant in eq 2. Model parameters were taken to represent chitosan solutions described in the Experimental Methods section such that the effects of changing the following parameters could be observed: (A) added salt concentration, c_{NaCl}, (B) fraction of deacetylation f_D, (C) concentration of chitosan represented by concentration of glucosamine monomer c_g at 25 °C, and (D) temperature T. (The relative permittivities of water used in the calculation were 86, 78, and 74 at 278, 298, and 310 K, respectively (values taken from Appendix 1.1 of ref 30)). $\bar{\psi}(r) = e\psi(r)/kT$ increases when α or f_D increase and when c_{NaCl} or the concentration of chitosan decrease while no significant change in the normalized potential occurs as a function of temperature under these solution conditions.

increase in the electrostatic potential for higher f_D (Figure 5B). This reduction in pK_{ap} with increasing f_D is larger without added salt (Figure 6). In contrast to the relatively slight effect of f_D on pK_{ap}, a much stronger influence of f_D on the degree of ionization at precipitation, α_p, was observed where chitosan with higher levels of deacetylation precipitated at higher degrees of ionization (Table 2). For example, for solutions without added salt, chitosan with $f_D = 0.98$ precipitated at $\alpha_p = 0.50$ while chitosan with $f_D = 0.72$ precipitated at $\alpha_p = 0.25$.

Table 2. Degree of Ionization of Chitosan at Precipitation, α_p, as Well as pK_0 and the Slope of pK_{ap} vs α, $\Delta pK_{ap}/\Delta\alpha$ or C_{cNaCl}, Measured at 25 °C for Different f_D Values and with Different NaCl Concentrations, c_{NaCl}

c_{NaCl} (mM)	f_D 0.72	f_D 0.85	f_D 0.98
	α_p[a] (±0.05)		
0	0.25[b]	0.30	0.50[b]
15	0.25	0.35	0.50
150	0.30	0.40	0.55
	pK_0^{PB} [c]		
0	6.63 ± 0.02	6.69 ± 0.01	6.78 ± 0.02
15	6.64 ± 0.01	6.67 ± 0.01	6.67 ± 0.01
150	6.73 ± 0.01	6.76 ± 0.01	6.75 ± 0.01
	pK_0^{lin} [d]		
0	6.63 ± 0.02	6.56 ± 0.03	6.40 ± 0.05
15	6.63 ± 0.01	6.57 ± 0.02	6.48 ± 0.02
150	6.70 ± 0.01	6.70 ± 0.02	6.71 ± 0.02
	$-\Delta pK_{ap}/\Delta\alpha^{PB}$ [e] (C_{cNaCl}^{PB})		
0	1.35 (0.014)	1.55 (0.017)	1.68 (0.04)
15	0.81 (0.011)	0.91 (0.01)	0.97 (0.011)
150	0.38 (0.002)	0.43 (0.008)	0.48 (0.009)
	$-\Delta pK_{ap}/\Delta\alpha^{lin}$ [f] (C_{cNaCl}^{lin})		
0	1.41 ± 0.01	1.46 ± 0.04	1.38 ± 0.04
15	0.87 ± 0.01	0.86 ± 0.03	0.88 ± 0.02
150	0.37 ± 0.01	0.38 ± 0.04	0.49 ± 0.02

[a] Calculation of α_p from experimental measurements ($n = 3$ with error of ±0.05 due to measurement accuracy). [b] Similar values were obtained at 5 and 37 °C with $n = 3$. [c] pK_0^{PB} are values of pK_0 obtained using $a = 1.3$ nm via the PB fit described in the "Determination of p$K_0(T)$ and of the Temperature-Induced Change in pK_{ap}" subsection. The error is represented as the standard deviation of the pK_0^{PB} fitted values ($n = 3$). [d] pK_0^{lin} are y-axis intercepts obtained from a linear fit of the experimental pK_{ap} values in the non-precipitated region and with $\alpha \leq 0.90$. The error is represented as the standard deviation of the pK_0^{lin} fitted values ($n = 3$). [e] $\Delta pK_{ap}/\Delta\alpha^{PB}$ are slope values obtained by a linear fit of the theoretical PB calculation in the non-precipitated region and with $\alpha \leq 0.90$ using $a = 1.3$ nm. The value in parentheses is a quality of fit parameter and corresponds to the root-mean-square of the difference between the experimental and fit (PB) pK_a values for the non-precipitated region. [f] $\Delta pK_{ap}/\Delta\alpha^{lin}$ are slope values obtained by a linear fit of the experimental pK_{ap} in the non-precipitated region and with $\alpha \leq 0.90$. The error is represented as the standard deviation of the slope fitted values ($n = 3$).

The intrinsic monomeric dissociation constant pK_0 at 25 °C obtained from linear fits of titration data (Figure 6) revealed a slight dependence on the concentration of added salt and f_D (pK_0^{lin} in Table 2). The lowest pK_0^{lin} (pK_0^{lin} = 6.40 at 25 °C) was found for chitosan ($f_D = 0.98$) without added salt, and the highest (pK_0^{lin} = 6.71 at 25 °C) for the same chitosan (f_D = 0.98) with 150 mM added salt.

The intrinsic pK_0 obtained from PB model fits (Figure 4), pK_0^{PB}, at 25 °C displayed less dependence than pK_0^{lin} on f_D and c_{NaCl}. We found no influence of f_D on pK_0^{PB} for a given amount of added salt while the values of pK_0^{PB} at c_{NaCl} = 150 mM were slightly higher than those at 0 or 15 mM added salt. An exception to these trends was seen with $f_D = 0.98$, c_{NaCl} = 0 mM, where the PB fit was not as good as that for other conditions (Figure 4). We found that a larger chitosan rod radius of $a = 1.5$ nm rather than 1.3 nm for $f_D = 0.98$, $c_{NaCl} = 0$ mM, resulted in a better fit and a value of pK_0 of 6.69, which is more consistent with pK_0 found for other conditions.

Nonlinearity and Convexity of the PB Model of p$K_{ap}(\alpha)$. The PB model (Figure 5) indicated that the normalized surface potential was typically greater than unity (with the exception of c_{NaCl} = 150 mM or small values of α) so that linearization

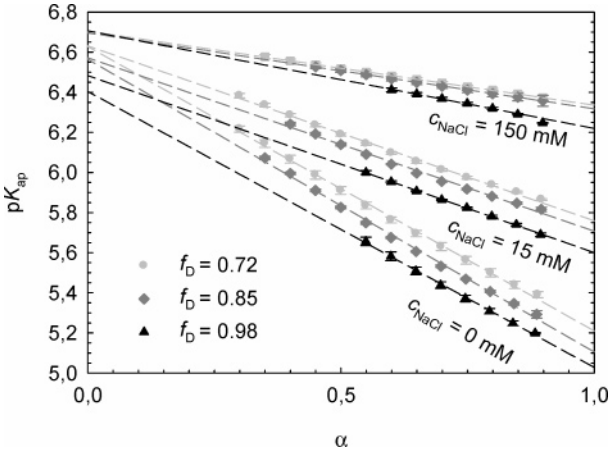

Figure 6. Dependence of chitosan pK_{ap} at 25 °C (mean ± SD, n = 3) on degree of ionization (α) for nine combinations of f_D and c_{NaCl}, directly comparing chitosans with different f_D values. Linear fits are shown as dashed lines. Solutions of chitosan with an initial concentration of glucosamine of 3 mM were titrated using 0.01 N NaOH, as described in the Experimental Methods section. Only data in the soluble non-precipitated region is shown to improve clarity. (See Figure 4 for data in precipitated regions.)

of the Poisson−Boltzmann equation would not be justified. Therefore a nonlinear variation of the potential with α is expected, particularly for low levels of added salt (0 and 15 mM). When using the PB model to calculate the surface potential $\psi|_{r=a}$ to obtain pH (eq 11) and pK_{ap} (eq 12) we found $\psi|_{r=a}$ to be a concave function of α such that its negative in the rightmost term of pK_{ap} (eq 12) was a convex function of α (Figure 7). The nonlinearity and convexity of pK_{ap}(α) was particularly pronounced for low-salt cases and when only the counterion was present (Figure 7A, 0 mM salt, no co-ions). The nonlinearity of pK_{ap}(α) was also visible in experimental curves at c_{NaCl} = 0 and 15 mM where we can see a slight convexity of titration curves, more easily observed for f_D of 0.72 and 0.85 since they have more data in the non-precipitated range (Figure 4). An important consequence of the nonlinearity of pK_{ap} versus α in our study was its ability to account for the discrepancy between pK_0 found by the nonlinear PB model (pK_0^{PB}) versus that found by linearly extrapolating experimental pK_{ap} from the non-precipitated region to α = 0 (pK_0^{lin}). The linearly extrapolated pK_0 (pK_0^{lin}) values were always lower than the pK_0 values from the PB model (pK_0^{PB}) (Figure 7). This difference was larger in the absence of added salt and when f_D was high and also when extrapolation was performed using a small number of experimental points, as expected because of the higher curvature of theoretical pK_{ap} curves at large f_D and low added salt (Figure 7). As an example, the largest difference was found between pK_0^{PB} and pK_0^{lin} (Table 2) when f_D = 0.98 and c_{NaCl} = 0 mM, with pK_0^{PB} = 6.78 versus pK_0^{lin} = 6.40, respectively, while an excess of salt with c_{NaCl} = 150 mM produced similar pK_0^{PB} and pK_0^{lin} values of 6.75 and 6.71, respectively.

Influence of Chitosan Concentration on pK_{ap}. The effect of chitosan concentration on chitosan pK_{ap} at 25 °C was tested by performing dilution experiments using a chitosan with f_D = 0.72 at α = 0.75. The pK_{ap} decreased significantly, by more than 0.4 units when diluting chitosan with deionized water from 30 to 3 mM glucosamine, whether salt was initially present or not (Figure 8A). On the contrary, adding excess salt to chitosan and diluting with excess salt at the same concentration had no effect on chitosan pK_{ap} (Figure 8A). Thus chitosan pK_{ap} depends strongly on chitosan concentration when either no salt is present or when changing chitosan concentration changes salt concentration due to the diluting solution. These results were also well

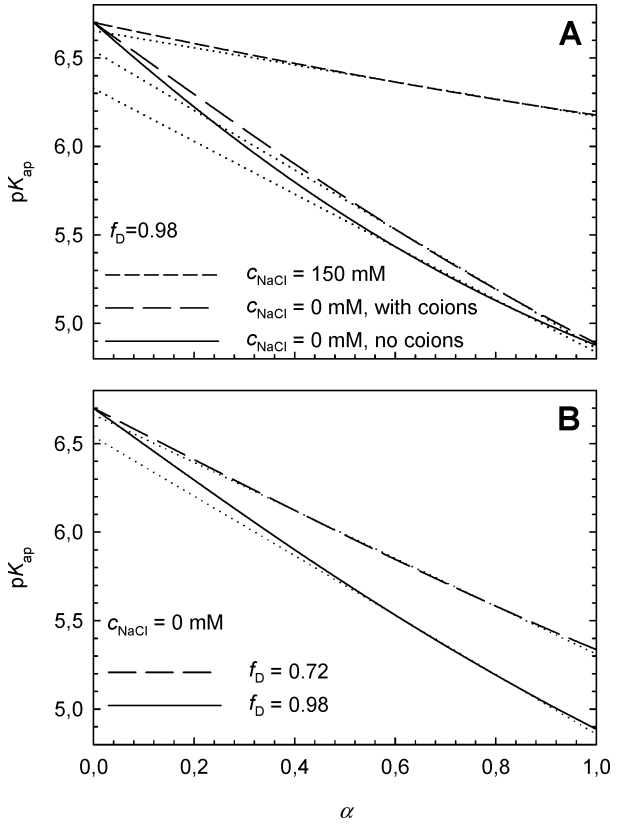

Figure 7. PB model (continuous and dashed lines) of pK_{ap} at 25 °C vs α compared to linear fits (the adjacent dotted lines) of the model in the non-precipitated region of experimental data (Figure 4 and Table 2) and with α ≤ 0.90. The PB model used pK_0 = 6.7, a = 1.3 nm, and a chitosan glucosamine monomer concentration of 3 mM. (A) Calculations with f_D = 0.98 for solutions containing (1) no salt and no co-ions with HCl adjusted to vary α, (2) no salt but with co-ions where HCl was constant at a molar ratio of HCl/glucosamine of 1:1 and NaOH was adjusted to vary α, and (3) as in 2 but with 150 mM NaCl present. The linear fits to the model were obtained in the ranges 0.55 < α < 0.90 and 0.6 < α < 0.90 without added salt and with 150 mM NaCl, respectively. The pK_0 obtained from linearly extrapolated regions of the PB model fall below the PB model due to nonlinearity and convexity of pK_{ap}(α) in the latter. (B) Comparison of chitosan with f_D values of 0.72 and 0.98 without added salt but with co-ions. The linear fits were obtained in the ranges 0.30 < α < 0.90 and 0.55 < α < 0.90 for f_D = 0.72 and f_D = 0.98, respectively.

described by PB model (Figure 8B) since dilution of chitosan increases surface potential $\psi|_{r=a}$ when salt is not in excess (Figure 5C) and thus expels protons from the chain to reduce pH, or equivalently pK_{ap}. Interestingly, the surface potential calculated from the PB model without added salt was linearly dependent on the logarithm of the glucosamine concentration in the range of 1−30 mM (inset in Figure 8B), consistent with previous observations.[31]

Temperature Dependence of pK_a of Glycerol Phosphate and Glucosamine and of pK_{ap} and α$_p$ of Chitosan. Temperature ramps that heated solutions from 5 to 40 °C were performed for two simple electrolytes, D-(+)-glucosamine and glycerol phosphate, as well as on chitosan solutions. pK_{ap} versus temperature was obtained from the measured pH according to eq 19 with T_{ref} = 5 °C (Figure 9). D-(+)-Glucosamine exhibited a strong variation of pK_a with a temperature of −0.027 ± 0.001 pK unit/°C (mean ± SD, n = 3), representing nearly a full unit decrease from 5 to 40 °C. In contrast the pK_a of glycerol phosphate was nearly invariant in the same temperature range. A similarly strong temperature dependence of glucosamine pK_a was observed previously by Neuberger[32] while the temperature-

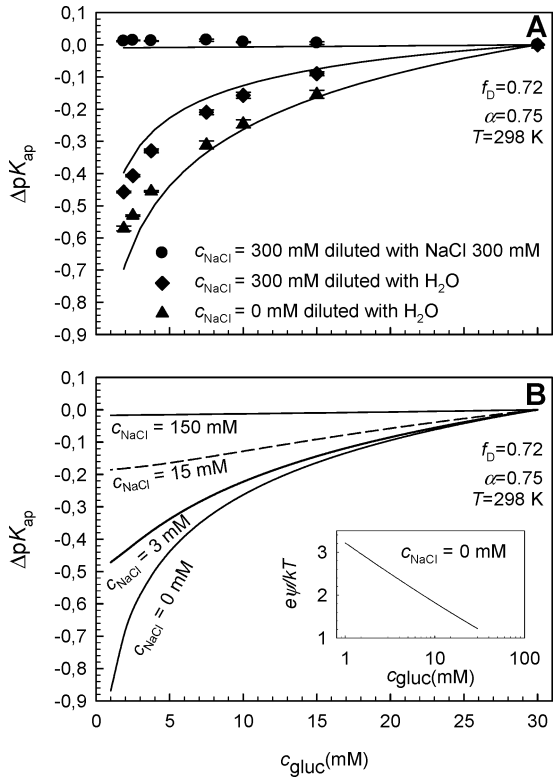

Figure 8. Dependence of chitosan pK_{ap} at 25 °C on chitosan concentration ($\Delta pK_{ap}(c_{gluc}) = pK_{ap}(c_{gluc}) - pK_{ap}(c_{gluc} = 30mM)$) represented as glucosamine monomer concentration. (A) Dilution of chitosan ($f_D = 0.72$) at a molar ratio of HCl/glucosamine monomer of 0.75:1. The PB model is shown as continuous lines. (B) PB model with $f_D = 0.72$ for chitosan with a molar ratio of HCl/glucosamine monomer of 0.75:1 and then diluted with various concentrations of NaCl, where the initial NaCl concentration in the chitosan solution was identical to that used for dilution.

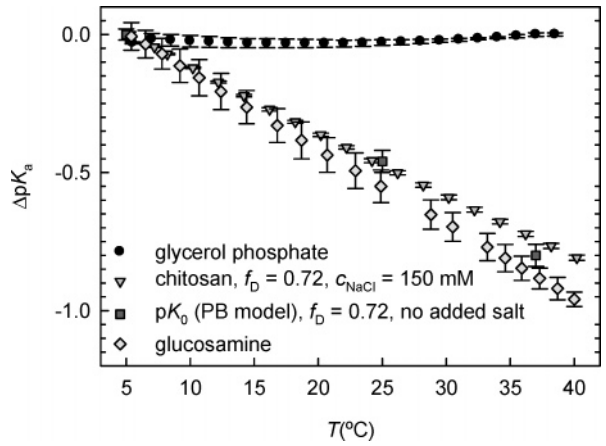

Figure 9. Temperature ramp tests revealing temperature dependence of pK_a of glycerol phosphate ($\alpha = 0.5$) and glucosamine ($\alpha = 0.95$) and pK_{ap} of chitosan (0.01 N NaOH added to obtain $\alpha = 0.75$), the latter with $f_D = 0.72$ and $c_{NaCl} = 150$ mM (from eq 19 with reference temperature 5 °C, showing mean ± SD, $n = 3$). The gray squares are PB model values of $\Delta pK_{ap} = pK_0^{PB}(T) - pK_0^{PB}(T_{ref})$ obtained from the PB model fits of pK_{ap} vs α titration measurements of chitosan at constant but different temperatures of 5, 25, and 37 °C (Figure 10) in the non-precipitated region and where $\alpha \leq 0.90$. pK_a of D-(+)-glucosamine and pK_{ap} of chitosan displays a significant decrease upon heating while pK_a of glycerol phosphate remained constant.

insensitive pK_a of glycerol phosphate was observed previously by Fukada.[33]

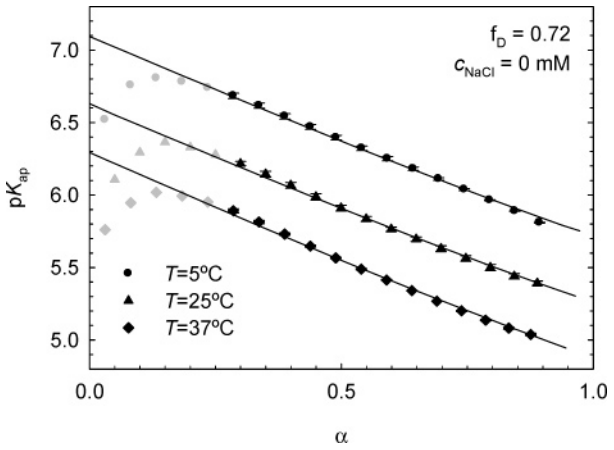

Figure 10. Chitosan ($f_D = 0.72$) pK_{ap} vs α (mean ± SD, $n = 3$) at constant but different temperatures of 5, 25, and 37 °C without added salt. Data obtained in the precipitated region are shown in gray, and PB model predictions as continuous lines.

Chitosan solutions with $f_D = 0.72$ and 150 mM NaCl at $\alpha = 0.75$ were also exposed to temperature ramps from 5 to 40 °C and chitosan pK_{ap} versus temperature obtained from the measured pH according to eq 19 with $T_{ref} = 5$ °C (Figure 9). The observed temperature dependence of chitosan pK_{ap} was slightly lower than that for glucosamine with a slope of -0.0232 ± 0.0003 pK unit/°C (mean ± SD, $n = 3$), indicating that this temperature-dependent ionization of chitosan arises mainly from the temperature dependence of its intrinsic monomeric dissociation constant p$K_0(T)$ in eqs 11 and 12. This conclusion was further confirmed by the negligible effect of temperature on the normalized potential ($e\psi/kT$) profile in the PB model (Figure 5D), eliminating any temperature-dependent contribution of the electrostatic contribution to chitosan pK_{ap} (i.e., $-e\psi|_{r=a}/kT$ ln 10 in eq 12 is temperature-independent). It is noteworthy that the temperature independence of the normalized potential in the PB model (Figure 5D) was due to the temperature dependence of water permittivity, which decreases with increasing temperature, resulting in a linearly increasing electrostatic potential and therefore a potential ($e\psi/kT$) normalized to temperature that was temperature-independent.

Chitosan titration experiments performed at different but constant temperatures (5, 25, and 37 °C in Figure 10) also showed a strong temperature dependence of chitosan pK_{ap} that was independent of α since increasing temperature vertically shifted pK_{ap} versus α and uniformly so for all values of α in the non-precipitated regions. The pK_0^{PB} values obtained from PB model fits of these latter titration measurements were used to calculate $\Delta pK_{ap} = pK_0(T) - pK_0(T_{ref})$ with $T_{ref} = 5$ °C (gray squares in Figure 9) and revealed a temperature dependence similar to pK_{ap} measured by temperature ramp tests of chitosan. In contrast to the strong temperature dependence of chitosan pK_{ap}, the degree of ionization of chitosan at precipitation, α_p, did not appear to depend on temperature according to experiments performed at 5, 25, and 37 °C with f_D of either 0.72 or 0.98 since α_p values at 25 °C were indistinguishable from those obtained at 5 and 37 °C (Table 2).

Discussion

The primary objective of the current study was to examine chitosan ionization and precipitation behavior as a function of ionic strength, fraction of deacetylation (f_D), chitosan concentration, and temperature and to assess the ability of the nonlinear

Poisson−Boltzmann cylindrical cell model to predict chitosan solution properties at finite chitosan concentration. We found that increasing salt (c_{NaCl}) strongly increased pK_{ap} (Figures 4 and 6) since increased electrostatic screening facilitated chain protonation[14] by reducing the chitosan surface potential and the magnitude of the polyelectrolyte term $-e\psi|_{r=a}/(kT \ln 10)$ in eq 12. Also as expected, chitosans with higher levels of deacetylation (higher f_D) bore a slightly increased surface charge density (eq 1) and therefore possessed slightly lower pK_{ap} values (Figures 5C and 6) due to an increased surface potential in eq 12. This lower chitosan pK_{ap} at higher f_D was similar to that observed in one prior study titrating chitosan in 100 mM $KClO_4$[14] but not as strong as that reported in another.[12] Both the level of deactylation (f_D) and concentration of added salt (c_{NaCl}) were found to influence the degree of chitosan ionization at which precipitation occurs (α_p), where α_p was increased for either an increase in f_D or c_{NaCl} (Table 2). Temperature had no discernible effect on α_p. Our finding that increased levels of deacetylation increased the degree of ionization at which precipitation occurs was opposite to our initially proposed hypothesis since we expected higher charge densities along the chain to increase electrostatic repulsion and impede interchain association to inhibit precipitation. However it appears that increasing the fraction of monomers bearing acetyl groups is effective at blocking interchain associations, possibly due to steric hindrance via these side groups and/or a more difficult alignment of the polymer chains with increasing amounts of acetyl groups, as suggested previously.[21] In any case, this reduced solubility of chitosan at higher f_D has been reported previously by several authors.[12,14,21]

We found that intrinsic monomeric dissociation constants, pK_0, obtained from linear extrapolations of pK_{ap}, using data in the soluble range of the chitosan degree of ionization ($\alpha > 0.3$ to 0.6 depending on f_D or c_{NaCl}, Figure 4); i.e., pK_0^{lin} ranged from 6.4 to 6.7, while those obtained from PB model fits, i.e., pK_0^{PB}, ranged from 6.63 to 6.78. The larger range in the linearly extrapolated values was due to the linear extrapolation failing to follow the convexity and nonlinearity of the PB model for pK_{ap} versus α (Figure 7). Nonetheless, this nonlinearity and convexity of the PB model was eliminated in the presence of excess salt (150 mM) such that linearly extrapolated pK_0^{lin} agreed with the PB model pK_0^{PB} (Figure 7) to provide pK_0 in the range from 6.70 to 6.76 and independent of f_D. This range of values of chitosan pK_0 (6.70−6.76) agrees with a previously reported pK_0 of 6.74 that was extrapolated from titrations performed on chitosans oligomers of increasing lengths.[16] The latter method bears the advantage of oligomer solubility over the entire range or ionization. In contrast to the close agreement between our pK_0 values and those of Tsukada,[16] there is significant variability of the previously reported chitosan pK_0 values, ranging from 6.0 to 9.0.[12,14−19] The two studies that reported chitosan pK_0 near 9[15,19] are not compatible with our results nor with those of several other studies,[12,14,16−18] possibly due to a sign error in the pK_{ap} equation that was used, i.e., pK_{ap} = pH − $\log_{10}(\alpha/(1-\alpha))$[19] or p$K_{ap}$ = pH + $\log_{10}((1-\alpha)/\alpha)$[15] rather than p$K_{ap}$ = pH + $\log_{10}(\alpha/1-\alpha)$ where α is the fraction of protonated glucosamine monomer on the chain. We estimated that correction of the sign error in refs 19 and 15 would result in chitosan pK_0 values in the range of 6.5 to 7.0. Another previous study[17,18] found chitosan pK_0 values to be 6.0 in both acetic acid and hydrochloric acid. This value appears low compared to our range from 6.70 to 6.76 and may be inaccurate due to pH measurements occurring at a low degree of ionization where chitosan is partly insoluble. Our range of obtained chitosan pK_0 values of 6.70−6.76 in 150 mM NaCl is however relatively close to those of Sorlier et al.[14] and Domard[12] who found pK_0 values of 6.5 for chitosans with f_D values similar to those tested in our study. We found salt to have a slight effect on pK_0^{PB} where values at $c_{NaCl} = 0$ and 15 mM were slightly lower by ~0.1 unit than at $c_{NaCl} = 150$ mM (Table 2). However, pK_0^{PB} values were independent of f_D (Table 2), suggesting that intramolecular interactions have negligible effects on pK_0. One possible exception to the latter is the case $f_D = 0.98$, $c_{NaCl} = 0$ mM, where p$K_0^{PB} = 6.78$ was slightly higher than that for other f_D values (Table 2) but for which the PB fit using $a = 1.3$ nm was also not as good as that for the other conditions (Figure 4).

We found that the accuracy of the potentiometric titration of chitosan was improved by taking the following precautions: (1) The chitosan used should be of high purity and thoroughly dried, or the water content should be precisely known (2) f_D should also be precisely known and should preferably be measured by ^{1}H NMR[34] (3) the occurrence of precipitation during titration should be detected by a sensitive method, rather than by visual inspection, to ensure valid analysis of the results that depend on solution homogeneity and (4) the determination of pK_0 of chitosan by linear extrapolation in solutions without added salt should be avoided. A particular limitation of our study was a variable molecular weight (MW) between chitosans with different f_D values. Ideally all of our chitosans would have had the same MW. However, even with the variable MWs of the three chitosans used, it is reasonable to assume that all are sufficiently long (length > ~600 monomers) so as to not allow size to influence the surface potential of the polymer in a soluble state. However, the MW could possibly influence the charge state at which precipitation occurs, as it is expected that at constant f_D precipitation of higher MW chitosan could occur at a higher α than for a shorter chain.

A novel finding in our study was the significant influence of chitosan concentration on chitosan pK_{ap} without added salt while for excess added salt no influence of chitosan concentration on chitosan pK_{ap} was observed (Figure 8A). These effects were accurately predicted by the PB model (Figure 8A) and were similar to those reported previously by Nitta and Sugai[31] and by Katchalsky et al.[35] for other polyelectrolytes. The influence of chitosan concentration on ionization behavior should be kept in mind, particularly when reporting pK_{ap} values of chitosan solutions without added salt.

We discovered in the current study that increasing temperature strongly reduced the apparent pK_a of chitosan, pK_{ap}, by ~0.023 pK_a units per °C, in a manner that is very similar to the temperature dependence of pK_a of monomeric glucosamine (Figures 9 and 10). This similar behavior for pK_{ap} of chitosan and pK_a of glucosamine strongly suggested this effect to be mediated by the intrinsic monomeric dissociation constant of chitosan p$K_0(T)$ in eq 12 rather than the polyelectrolyte term $-e\psi|_{r=a}/(\ln 10\ kT)$ in eq 12. This conclusion was supported by the PB model, which predicted a negligible variation of the normalized electrostatic potential with temperature (Figure 6A) when the dependence of water permittivity on temperature was included.

The Poisson−Boltzmann cylindrical cell model was remarkably successful in providing molecular level insight and interpretation of all of the above findings. We found that this PB model using a polyelectrolyte radius a of 1.3 nm accurately predicted the dependence of chitosan pK_{ap} on f_D, salt, chitosan concentration, and temperature (Figures 4, 6, 8, 9, and 10). While polyelectrolyte titrations have been modeled using several approaches[22,36−40] (see Ullner[41] for a review), we used the mean-

field Poisson−Boltzmann cylindrical cell model, since the chitosan persistence length is about 10−15 nm,[29,42−45] suggesting that the chain is stiff enough[46] to apply this model. We set the radius of the impenetrable inner cylinder to $a = 1.3$ nm, which is greater than the crystallographic structural parameter (0.42 nm),[24] yet appears most appropriate since all pK_{ap} curves obtained at 25 °C could be described well using $a = 1.3$ nm. Furthermore, a value of the rod radius that is greater than the structural value is often used in the cylindrical PB model to describe polyelectrolyte data.[22,31,36] It should be noted that PB model fits under low-salt conditions were more sensitive to the choice of the a value since much higher electrostatic potentials occur. Even though the PB model is generally nonlinear, a useful simplification of eq 7 that reasonably predicts pK_{ap} at least in the non-precipitated range is $pK_{ap} = pK_0 - C_T(T - T_{ref}) - C_{cNaCl}\alpha$ where we found $C_T = 0.023$/°C (Figures 9 and 10) to be independent of c_{NaCl} and f_D while $C_{cNaCl}(c_{NaCl},f_D)$ and pK_0-(T_{ref},c_{NaCl},f_D) do depend on the concentration of added salt (c_{NaCl}) and f_D as shown in Table 2 at $T_{ref} = 25$ °C. For temperature-dependent measurements, the ability of the pH probe to compensate for temperature is important and care should be taken to test pH accuracy versus temperature. Also, results obtained in this paper show that α is a more appropriate parameter than pH to characterize precipitation or solubility, as suggested by Siegel and Cornejo-Bravo,[47] since α is the ionization state of the polyelectrolyte and is a primary determinant of solubility. In contrast pH can be strongly influenced by temperature and the presence and dissociation of other solution components that may or may not influence precipitation.

For the temperature range from 5 to 40 °C, we found that the pK_a of glucosamine and the pK_0 of chitosan decrease significantly with temperature by −0.027 and −0.023 pK units/°C, respectively, while the pK_a of glycerol phosphate was found to be temperature-independent. Gurney[48] proposed the following relation for the temperature variation of proton dissociation constants of noncharged and negatively charged acids

$$\log_{10}(K_a) = -C\frac{(A + \exp(T/\theta))}{T} \qquad (20)$$

where C and A are characteristic of the acid and θ is a parameter that depends only on the solvent. For positively charged acids such as chitosan and glucosamine, proton dissociation is free from any work necessary to separate two charged species in solution, and the contribution of the $\exp(T/\theta)$ term, which contains the effects of the dielectric constant of the solvent, is negligible.[49] Thus, chitosan and glucosamine are expected to show a linear variation of pK_a versus $1/T$, and the relationship of Gurney is simply

$$pK_a = \frac{CA}{T} = \frac{D}{T} \qquad (21)$$

Using a pK_0 of 6.6 (Table 2) for chitosan and a pK_a of 7.8[13] for glucosamine at $T = 298$ K in eq 21, we found that $D = 1967$ K^{-1} for chitosan and $D = 2324$ K^{-1} for glucosamine. For chitosan, calculation of the pK_0 at 278 and 313 K gives 7.08 and 6.28, respectively, corresponding to an average variation of −0.0227 pK units/°C for the range of 5−40 °C. For glucosamine, the same calculation gives an average variation of −0.0267 pK units/°C for the range of 5−40 °C. These calculated values are very close to the experimental values found in our study of −0.0232 ± 0.0003 pK units/°C for chitosan and −0.027 ± 0.001 pK units/°C for glucosamine.

The marked influence of temperature on chitosan pK_{ap} values (Figures 9 and 10) and the corresponding temperature insensitivity of the pK_a values of glycerol phosphate (Figure 9) sheds light on the molecular mechanism of heat-induced gelation of these systems that has been reported previously.[10] Heating of chitosan significantly reduces its pK_{ap} value, thus producing a tendency for chitosan amine groups to release protons and become neutralized, as would occur if base were added. However, chitosan can release protons and become neutralized upon heating only if a proton acceptor is present in solution. Glycerol phosphate is an ideal proton acceptor since its proton equilibrium is not affected by heating, and its pK_a is close to the chitosan pK_{ap}. We therefore expect a net transfer of protons from chitosan to glycerol phosphate to reduce α with heating, thereby neutralizing chitosan in solution in a spatially uniform manner that allows for bulk gelation in sufficiently concentrated solutions. One would expect multiple parameters to influence this gelation process including: (1) the amount of HCl present where lower amounts reduce the initial α to gel at lower temperature, as observed previously,[10] and (2) the amount of glycerol phosphate where higher amounts will also reduce the initial α and more efficiently accept protons such that chitosan will gel at lower temperature, also as observed previously.[10] An additional critical factor expected from our study is the degree of deacetylation, which strongly affects solubility via its influence on α_p (Table 2). Studies are ongoing where the current model is elaborated to explicitly account for other titratable species in solution, such as glycerol phosphate, and to include the dependence of the degree of ionization of chitosan at precipitation (α_p) on ionic strength and degree of deacetylation to provide a complete model able to predict gelation behavior and design specific systems with desired solubility, ionization, and thermosensitive characteristics.

Acknowledgment. This work was supported by the Natural Sciences and Engineering Research Council of Canada. M.L. received a doctoral fellowship from the Canadian Institutes of Health Research. D.F. received a doctoral fellowship from le Fonds de Recherche sur la Nature et les Technologies Québec.

Supporting Information Available. Derivation of the pH dependence on the electrostatic potential (eq 11) and derivation of $dpK_{ap} \cong dpH$ (eq 16). This information is available free of charge via the Internet at http://pubs.acs.org.

References and Notes

(1) Hoppe-Seyler, F. *Ber. Dtsch. Chem. Ges.* **1894**, *27*, 3329−3331.
(2) Chenite, A.; Chaput, C.; Wang, D.; Combes, C.; Buschmann, M. D.; Hoemann, C. D.; Leroux, J. C.; Atkinson, B. L.; Binette, F.; Selmani, A. *Biomaterials* **2000**, *21*, 2155−61.
(3) Hirano, S.; Seino, H.; Akiyama, Y.; Nonaka, I. *Progress in Biomedical Polymers*, Proceedings of an American Chemical Society Symposium; Gebelein, C. G., Dunn, R. L., Eds.; American Chemical Society: Washington, DC, 1990; pp 283−290.
(4) Knapczyk, J.; Krowczynski, L.; Pawlik, B.; Liber, Z. In *Chitin and Chitosan: Sources, Chemistry, Biochemistry, Physical Properties, and Applications*; Skjåk-Braek, G., Anthonsen, T., Sandford, P., Eds.; Elsevier Applied Science: London, 1989; pp 665−669.
(5) Lavertu, M.; Methot, S.; Tran-Khanh, N.; Buschmann, M. D. *Biomaterials* **2006**, *27*, 4815−4824.
(6) Liu, W. G.; Yao, K. D. *J. Controlled Release* **2002**, *83*, 1−11.
(7) MacLaughlin, F. C.; Mumper, R. J.; Wang, J.; Tagliaferri, J. M.; Gill, I.; Hinchcliffe, M.; Rolland, A. P. *J Controlled Release* **1998**, *56*, 259−272.
(8) Muzzarelli, R. A. A.; Mattioli-Belmonte, M.; Pugnaloni, A.; Biagini, G. *EXS* **1999**, *87*, 251−264.
(9) Ueno, H.; Yamada, H.; Tanaka, I.; Kaba, N.; Matsuura, M.; Okumura, M.; Kadosawa, T.; Fujinaga, T. *Biomaterials* **1999**, *20*, 1407−14.
(10) Chenite, A.; Buschmann, M.; Wang, D.; Chaput, C.; Kandani, N. *Carbohydr. Polym.* **2001**, *46*, 39−47.
(11) Hoemann Caroline, D.; Hurtig, M.; Rossomacha, E.; Sun, J.; Chevrier, A.; Shive Matthew, S.; Buschmann Michael, D. *J. Bone Jt. Surg.* **2005**, *87*, 2671−2686.

(12) Domard, A. *Int. J. Biol. Macromol.* **1987**, *9*, 98−104.
(13) Park, J. W.; Choi, K. H.; Park, K. K. *Bull. Korean Chem. Soc.* **1983**, *4*, 68−72.
(14) Sorlier, P.; Denuziere, A.; Viton, C.; Domard, A. *Biomacromolecules* **2001**, *2*, 765−772.
(15) Strand, S. P.; Tommeraas, K.; Varum, K. M.; Ostgaard, K. *Biomacromolecules* **2001**, *2*, 1310−1314.
(16) Tsukada, S.; Inoue, Y. *Carbohydr. Res.* **1981**, *88*, 19−38.
(17) Rinaudo, M.; Pavlov, G.; Desbrieres, J. *Int. J. Polym. Anal. Charact.* **1999**, *5*, 267−276.
(18) Rinaudo, M.; Pavlov, G.; Desbrieres, J. *Polymer* **1999**, *40*, 7029−7032.
(19) Anthonsen, M. W.; Smidsroed, O. *Carbohydr. Polym.* **1995**, *26*, 303−5.
(20) Rinaudo, M.; Domard, A. In *Chitin and Chitosan: Sources, Chemistry, Biochemistry, Physical Properties, and Applications*; Skjåk-Braek, G., Anthonsen, T., Sandford, P., Eds.; Elsevier Applied Science: London, 1989; pp 71−86.
(21) Varum, K. M.; Ottoy, M. H.; Smidsrod, O. *Carbohydr. Polym.* **1994**, *25*, 65−70.
(22) Kotin, L.; Nagasawa, M. *J. Chem. Phys.* **1962**, *36*, 873−879.
(23) Marcus, R. A. *J. Chem. Phys.* **1955**, *23*, 1057−1068.
(24) Mazeau, K.; Winter, W. T.; Chanzy, H. *Macromolecules* **1994**, *27*, 7606−7612.
(25) Okuyama, K.; Noguchi, K.; Miyazawa, T.; Yui, T.; Ogawa, K. *Macromolecules* **1997**, *30*, 5849−5855.
(26) Buschmann, M. D.; Grodzinsky, A. J. *J. Biomech. Eng.* **1995**, *117*, 179−192.
(27) Carnie, S. L.; Torrie, G. M. *Adv. Chem. Phys.* **1984**, *56*, 141−253.
(28) Fixman, M. *J. Chem. Phys.* **1979**, *70*, 4995−5005.
(29) Brugnerotto, J.; Desbrieres, J.; Roberts, G.; Rinaudo, M. *Polymer* **2001**, *42*, 09921−09927.
(30) Robinson, R. A.; Stokes, R. H. *Electrolyte Solutions*, Dover: New York, 2nd revised ed.; 2002.
(31) Nitta, K.; Sugai, S. *J. Phys. Chem.* **1974**, *78*, 1189−93.
(32) Neuberger, A.; Fletcher, A. P. *J. Chem. Soc. B* **1969**, *2*, 178−81.
(33) Fukada, H.; Takahashi, K. *Proteins: Struct., Funct., Genet.* **1998**, *33*, 159−166.
(34) Lavertu, M.; Xia, Z.; Serreqi, A. N.; Berrada, M.; Rodrigues, A.; Wang, D.; Buschmann, M. D.; Gupta, A. *J. Pharm. Biomed. Anal.* **2003**, *32*, 1149−1158.
(35) Katchalsky, A.; Shavit, N.; Eisenberg, H. *J. Polym. Sci.* **1954**, *13*, 69−84.
(36) Cleland, R. L.; Wang, J. L.; Detweiler, D. M. *Macromolecules* **1982**, *15*, 386−95.
(37) Borukhov, I.; Andelman, D.; Borrega, R.; Cloitre, M.; Leibler, L.; Orland, H. *J. Phys. Chem. B* **2000**, *104*, 11027−11034.
(38) Nishio, T. *Biophys. Chem.* **1994**, *49*, 201−14.
(39) Smits, R. G.; Koper, G. J. M.; Mandel, M. *J. Phys. Chem.* **1993**, *97*, 5745−5751.
(40) Ullner, M.; Joensson, B.; Soederberg, B.; Peterson, C. *J. Chem. Phys.* **1996**, *104*, 3048−3057.
(41) Ullner, M. In *Handbook of Polyelectrolytes and Their Applications*; Tripathy, S. K., Kumar, J., Nalwa, H. S., Eds.; American Scientific Publisheres: Stevenson Ranch, CA, 2002; Vol. 3, pp 271−308.
(42) Anthonsen, M. W.; Varum, K. M.; Smidsrod, O. *Carbohydr. Polym.* **1993**, *22*, 193−201.
(43) Berth, G.; Dautzenberg, H.; Peter, M. G. *Carbohydr. Polym.* **1998**, *36*, 205−216.
(44) Rinaudo, M.; Milas, M.; Le Dung, P. *Int. J. Biol. Macromol.* **1993**, *15*, 281−285.
(45) Schatz, C.; Viton, C.; Delair, T.; Pichot, C.; Domard, A. *Biomacromolecules* **2003**, *4*, 641−648.
(46) Mandel, M. *J. Phys. Chem.* **1992**, *96*, 3934−3942.
(47) Siegel, R. A.; Cornejo-Bravo, J. M. In *Polyelectrolyte Gels: Properties, Preparation, and Applications*; Harland, R. S., Prud'homme, R. K., Eds.; ACS Symposium Series 480; American Chemical Society: Washington, DC, 1992; pp 131−145.
(48) Gurney, R. W. *Ionic Processes in Solution*; McGraw-Hill: New York, 1953.
(49) Tanaka, M.; Nomura, H.; Kawaizumi, F. *Bull. Chem. Soc. Jpn.* **1992**, *65*, 410−414.
(50) Bockris, J. O. M.; Reddy, A. K. N. *Modern Electrochemistry*, 2nd ed.; Plenum Press: New York, 1998; Vol. 1.

BM700520M